

An Investigation of a Gas

Cyclone for Size Classification

of Micropulverized Lignite

**An Investigation of A Gas Cyclone for Size Classification
of Micropulverized Lignite**

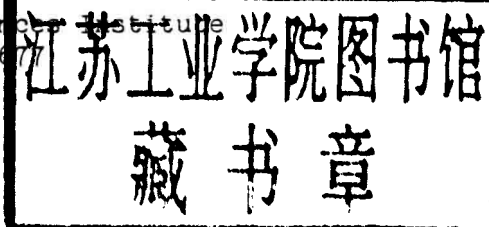
A Technical Report

by

Guy B. Spikes
and
Charles W. Bouchillon

Submitted to:

The Mississippi Mineral Resources Institute
University, MS 38677



Submitted by:

The Department of Mechanical & Nuclear Engineering
Mississippi State University
Mississippi State, MS 39762

July 1985

Open-File Report 85-2Sb

An Investigation of a Gas Cyclone for Size Classification
of Micropulverized Lignite

Gary B. Spikes and Charles W. Bouchillon

1985

The Mississippi Mineral Resources Institute
University, Mississippi 38677

MSU Publication Notice

Mississippi State University does not discriminate on the basis of race, color religion, national origin, sex, age, or handicap.

In conformity with Title IX of the Education Amendments of 1972 and Section 504 of the Rehabilitation Act of 1973, Joyce B. Giglioni, Assistant to the President, 610 Allen Hall, P. O. Drawer J, Mississippi State, Mississippi 39762, office telephone number 215-3221, has been designated as the responsible employee to coordinate efforts to carry out responsibilities and make investigation of complaints relating to discrimination.

ACKNOWLEDGMENTS

Sincere appreciation is expressed to the Engineering and Industrial Research Station and to the Tramel Computing Center at Mississippi State University for their financial and service support in the successful conduct of this project.

Thanks are also due Mr. M. J. Hibbard for specific advice concerning the use of the UNIVAC system.

Continuing financial support from the Mississippi Minerals Research Institute for research on processes for improving the quality of Mississippi lignites as a future source of energy is gratefully acknowledged. Work on this project was conducted largely through the support of MMRI Grant No. 85-2S.

An Investigation of a Gas Cyclone for Size Classification
of Micropulverized Lignite

by

Guy B. Spikes
and
Charles W. Bouchillon

ABSTRACT

A fundamentally based mathematical model of the gas flow and particle motion occurring in two types of gas cyclone separators was investigated. A conventional cylinder-on-cone-type cyclone with a single tangential gas inlet was first examined. Attention was then focused on an adjustable classifier-type cyclone having an auxiliary gas inlet in its conical base.

The equations describing the turbulent, confined vortex flow patterns in cyclone separators are the time-averaged continuity and momentum equations. A computer program was obtained and modified to solve this set of coupled, nonlinear, elliptic partial differential equations. The program also generates particulate grade-efficiency curves by solving the equations of motion of a number of discrete particles entrained in the predicted gas field. The effect of the turbulent fluid eddies on the motion of the particles was modeled using a stochastic technique.

The program was originally developed to predict the performance of a cylinder-on-cone-type cyclone. It was then modified in this study to model the classifier-type cyclone. The equations describing the flow

patterns in both type cyclone designs are identical and only the boundary conditions of the original problem need be revised to model the classifier-type cyclone designs.

The computer program was found to accurately predict the flow field and particulate collection efficiency in the cylinder-on-cone cyclone. The solution of the flow field equation for the classifier cyclone, however, exhibited some numerical instability. The limitations of the computer program and possible sources of the instability are discussed. Recommendations are made for improving and extending the model.

NOMENCLATURE

English Letters

A	area
a	coefficient in the discretization equation; also height of cyclone inlet (Figure 1.1)
b	width of cyclone inlet zone (Figure 1.1); also constant term in discretization equation 3.49
C_1	constant in approximate ϵ transport equation 2.12
C_2	constant in approximate ϵ transport equation 2.12
C_3	constant in transport equation for R_1 , equation 3.6
C_D	constant in S_D coefficient of turbulent kinetic energy equation (Table 3.1)
C_d	drag coefficient of solid particles
C_i	convective flux at $i = n, s, e$, and w control-volume faces
C_u	constant coefficient from the $k-\epsilon$ turbulence model
D	diameter of cyclone (Figures 1.1 and 5.1)
D_e	diameter of cyclone vortex finder outlet (Figure 1.1 or 5.1)
D_h	diameter of cyclone collection hopper (Figure 1.1 or 5.1)
D_p	diameter of solid particles
d	coefficient of pressure-difference term, equations 3.42
E	constant in the law of the wall
F	solid particle drag force, equation 2.23
F_i	strength of convection through control-volume face $i (= n, s, e, w)$
f_x	fraction of total volumetric flow rate into the cyclone that enters at the auxiliary inlet
G	generation of turbulence energy
H	overall cyclone height (Figure 1.1 or 5.1)
h	height of cyclone cylindrical body (Figure 1.1 or 5.1)

h_c	height of cyclone conical base (Figure 1.1 or 5.1)
h_x	height of lower auxiliary boundary of modified cyclone (Figure 5.1)
K_i	one-half the skew flux at control-volume face i ($= n, s, e, w$)
k	turbulent kinetic energy [$= 1/2(\overline{u'^2 + v'^2 + w'^2})$]
L_i	one-half the mass flux at control-volume face i ($= n, s, e, w$)
l	length scale of turbulence
\dot{m}	mass rate of flow
P	pressure
P'	pressure correction
Q	volume rate of flow
Ri	turbulent Richardson number
R_m	normalized mass residual, equation 3.61
R_ϕ	summation of the absolute residual vectors for variable ϕ , equation 3.57
Re	relative Reynolds number, equation 2.24
$RESOR_\phi$	normalized residual for variable ϕ
r	radial coordinate direction and distance from symmetry axis
r_1, r_2	cone radius at lower and upper boundaries of auxiliary inlet (Figure 5.2)
S_p	coefficient of ϕ_p in linearized source term
S_u	constant part of linearized source term
$S_{\phi i}$	coefficient in the SUDS discretization equations 3.36, ($\phi = \bar{u}, \bar{v}$, $i = n, s, e, w$)
s	length of cyclone vortex finder (Figure 1.1 or 5.1)
t	time
\bar{u}	time mean component of axial velocity
u'	fluctuating component of axial velocity
$\sqrt{\overline{u'^2}}$	r.m.s. axial velocity fluctuation

u^+	dimensionless velocity ($\equiv \bar{u}/u_*$), equation 2.14
u_*	friction velocity
V	volume
\vec{v}	velocity vector ($\bar{u}, \bar{v}, \bar{w}$)
VS_1	viscosity coefficient associated with $\overline{u'v'}$, equation 3.11
VS_3	difference between r.m.s. radial and tangential velocity fluctuations ($\equiv \overline{v'^2} - \overline{w'^2}$)
\bar{v}	time mean component of radial velocity
v'	fluctuating component of radial velocity
$\sqrt{\overline{v'^2}}$	r.m.s. radial velocity fluctuation
\bar{w}	time mean component of tangential velocity
w'	fluctuating component of tangential velocity
$\sqrt{\overline{w'^2}}$	r.m.s. tangential velocity fluctuation
y^+	dimensionless length ($\equiv \rho y u_*/\mu$), equation 2.14
z	axial coordinate direction and distance from symmetry axis
z_1, z_2	axial distance to lower and upper boundaries of the auxiliary inlet (Figure 5.1)

Greek Letters

α	coefficient in algebraic stress equation model, equation 3.12
α_ϕ	under-relaxation parameter for ϕ
β	coefficient in algebraic stress equation model, equation 3.13
Γ	gradient diffusion coefficient
Δr	r-direction width of a control-volume
δr	r-direction distance between adjacent grid points
$\Delta z, \delta z$	similar to $\Delta r, \delta r$

ϵ	dissipation rate of turbulence energy
ζ	normally distributed random number
θ	angular coordinate direction orthogonal to r and z directions
κ	constant in the law of the wall, equation 2.13
Λ_i	diffusion coefficient at control-volume face i ($= n, s, e, w$)
λ	constant in equations for ϵ boundary conditions at the inflow boundaries
μ	molecular viscosity
μ_t	turbulent viscosity ($= \rho C_\mu k^2 / \epsilon$)
μ_{eff}	effective viscosity, equation 2.10 ($= \mu + \mu_t$)
ρ	fluid density
σ_ϵ	constant in approximate ϵ transport equation 2.12
σ_k	constant in approximate k transport equation 2.11
τ	shear stress; also lifetime of a fluid eddy, equation 2.29
ϕ	general dependent variable

FORTRAN Variables

ALAMDA	λ , constant in equation for ϵ at inflow boundaries (Table 6.2)
ALNGTH	H , overall cyclone height (Table 6.2)
AUX	logical flag, set 'TRUE' if auxiliary inlet included in cyclone
CAPPA	κ , constant in the law of the wall (Table 6.2)
CD	C_D , constant in S_p coefficient of turbulent kinetic energy equation (Table 6.2)
CF	constant in shear stress equation for upper and lower surfaces of vortex finder (Table 6.2)
CMU	C_μ , constant in k - ϵ turbulence model (Table 6.2)
CONE	h_c , height of cyclone conical base (Table 6.2)

CONEX	z_1 , axial distance to lower boundary of auxiliary inlet (Table 6.3)
C1,C2	C_1, C_2 , constants in approximate ϵ transport equation (Table 6.2)
C3	C_3 , constant in transport equation for R_1 (Table 6.2)
DIAMTR	D , cyclone diameter (Table 6.2)
EFF	overall cyclone collection efficiency
ELOG	E , constant in the law of the wall (Table 6.2)
GEXPF	computational grid expansion factor
HIGHT	a , height of cyclone main inlet zone (Table 6.2)
HOPPER	D_h , diameter of cyclone collection hopper (Table 6.2)
I	grid point axial coordinante
IAXL	grid point location of lower boundary of auxiliary inlet (Figure 5.3)
IAXLP1	$IAXL + 1$
IAXU	grid point location of upper boundary of auxiliary inlet (Figure 5.3)
IAXUP1	$IAXU + 1$
INJECT	number of particle injection points
IPOINT	axial grid point location of main inlet zone (Figure 3.1)
ISTEP	axial grid point location of vortex finder (Figure 3.1)
IWALL	axial grid point location of cone/cylindrical wall interface (Figure 3.1 or 5.3)
J	grid point radial coordinante
JBGIN	radial grid point location of collection hopper (Figure 5.3)
JPOINT	radial grid point location of main inlet zone (Figure 3.1)
JSTEP	radial grid point location of vortex finder (Figure 3.1)
MAXIT	upper limit of flow field iteration counter
NI	total number of grid points in the axial direction (Figure 3.1)

NJ	total number of grid points in the radial direction (Figure 3.1 or 5.1)
NSIZES	number of sizes of particles tracked
NTOTAL	total number of particles tracked by mean or random particle tracking routines
NTRIES	number of tracks of a given particle size injected at a given point (= 1 for mean tracking)
SIGMAE	constant in approximate ϵ transport equation (Table 6.2)
SIGMAK	constant in approximate k transport equation (Table 6.2)
RHOP	ρ_p , solid particle density
TOTAL	total number of particles collected
TURBNX	turbulence intensity at auxiliary boundary (Table 6.3)
VORTEX	s , length of cyclone vortex finder (Table 6.2)

Subscripts

E	value at positive z-direction (east) neighbor grid point
e	control-volume face between P and E
i	value at i th axial grid point; also, value at main inlet boundary
j	value at j th radial grid point
N	value at positive r-direction (north) neighbor grid point
n	control-volume face between N and P
o	value at beginning of time interval
P	value at central grid point under consideration
p	value associated with a solid particle
r	$\partial/\partial r$, derivative with respect to r (Table 3.1)
S	value at negative r-direction (south) neighbor grid point
s	control-volume face between P and S

W	value at negative z -direction (west) neighbor grid point
w	control-volume face between W and P , also denotes wall value in Chapter II
x	value at the boundary of the auxiliary inlet
z	$\partial/\partial z$, derivative with respect to z (Table 3.1)

Superscript

$*$	previous-iteration value of a variable; also, velocities based on guessed pressure field (P^*)
-----	--

Special Symbols

$\max[A,B,C,\dots]$	largest of A,B,C,\dots
$\min[A,B,C,\dots]$	smallest of A,B,C,\dots

Table of Contents

Title Page	i
MSU Publication Notice	ii
Acknowledgments	iii
Abstract	iv
Table of Contents	vi
List of Figures	viii
List of Tables	x
Nomenclature	xi
Chapter I. Introduction	1
Chapter II. Formulation of the Problem	7
2.1 Time-Averaged Equations of the Flow Field	7
2.2 The Turbulence Closure Model	9
2.3 Boundary Conditions	13
2.4 Equations of Motion of the Solid Particles	13
Chapter III. Solution of the Differential System	20
3.1 The General Differential Equation	20
3.2 Discretization of the Equations	25
3.3 The Pressure-Correction Equation and SIMPLE Algorithm ..	36
3.4 Boundary Condition Implementation	40
3.5 Solution of the Discretization Equations	47
Chapter IV. Program Structure and Execution	53
4.1 Overall Structure	53
4.2 Calculation of the Flow Field	57
4.3 Calculation of the Particle Trajectories	60
Chapter V. Problem Modifications	68
5.1 The Modified Problem	68
5.2 Modification of the Computer Code	72
Chapter VI. Results and Conclusions	77
6.1 Modeling Cyclone A	77
6.2 Modeling Cyclone B	92
6.3 Conclusions	102
6.4 Recommendations	107

Appendix A. Computer Program	110
A.1 Description of the Program	111
A.2 Program Subroutine Index	114
Appendix B. Sample Output	117
B.1 Cyclone B: Particle Collection Efficiencies	118
B.2 Cyclone B: Flow Field	119
Bibliography	129

List of Figures

Figure	Description	Page
1.1	Cyclone Geometry	2
1.2	Sketch of Tangential Velocity Profile in a Vortex Chamber as Reported by Reydon and Gauvin [4]	4
2.1	Sketch of the Composition of Turbulent Flow Properties	7
2.2	Cyclone Coordinate System and Velocity Vectors	10
2.3	Solution Domain Boundaries	13
2.4	Near-Wall Grid Point and Control-Volume	14
2.5	Drag Coefficient for a Spherical Particle vs. Reynolds Number	17
3.1	Control-Volumes and Grid Points for a Uniform Grid	28
3.2	Control-Volume and Grid Point Cluster	29
3.3	Piecewise-Linear Profile Assumption (Axial Profile Shown)	33
3.4	Top Wall Boundary Control-Volume and Grid Point Cluster	44
3.5	Boundary Control-Volume for the Pressure-Correction Equation	47
3.6	Visualization of the Line-By-Line Method	48
4.1	Overall Flow Diagram	55
4.2	Typical Residuals Display	57
4.3	Flow Diagram for Solution of the Flow Field	58
4.4	Flow Diagram for Particle Tracking	61
5.1	Modified Cyclone Geometry	69
5.2	Differential Control-Volume in the Auxiliary Inlet	70
5.3	Grid Point Location of the Auxiliary Boundary	74